

Monte Carlo simulations of the four-dimensional XY spin glass at low temperatures

Helmut G. Katzgraber* and A. P. Young†

Department of Physics, University of California, Santa Cruz, California 95064

(Dated: November 6, 2018)

We report on the results for simulations of the four-dimensional XY spin glass using the parallel tempering Monte Carlo method at low temperatures for moderate sizes. Our results are qualitatively consistent with earlier work on the three-dimensional gauge glass as well as three- and four-dimensional Edwards-Anderson Ising spin glass. An extrapolation of our results would indicate that large-scale excitations cost only a finite amount of energy in the thermodynamic limit. The surface of these excitations may be fractal, although we cannot rule out a scenario compatible with replica symmetry breaking in which the surface of low-energy large-scale excitations is space filling.

PACS numbers: 75.50.Lk, 75.40.Mg, 05.50.+q

I. INTRODUCTION

There has been an ongoing controversy regarding the spin-glass phase. There are two main theories: the “droplet picture” (DP) by Fisher and Huse¹ and the replica symmetry breaking picture (RSB) by Parisi.^{2,3} While RSB follows the exact solution of the Sherrington-Kirkpatrick model and predicts that excitations which involve a finite fraction of the spins cost a finite energy in the thermodynamic limit, the droplet picture states that a cluster of spins of size l costs an energy proportional to l^θ , where θ is positive. It follows that in the thermodynamic limit, excitations that flip a finite cluster of spins cost an infinite energy. In addition, the DP states that these excitations are fractal with a fractal dimension $d_s < d$, where d is the space dimension, whereas in RSB these excitations are space filling,⁴ i.e., $d_s = d$.

Krzakala and Martin,⁵ as well as Palassini and Young⁶ (referred to as KMPY) found, on the basis of numerical results on small systems with Ising symmetry, that an intermediate picture may be present: while the surface of large-scale excitations appears to be fractal, only a finite amount of energy is needed to excite them in the thermodynamic limit. In the context of their work, it is necessary to introduce two exponents, θ and θ' , where L^θ is the typical energy for an excitation induced by a change in boundary conditions in a system of linear size L , and $L^{\theta'}$ describes the energy of thermally excited system-size clusters. Subsequently, similar results were found for the three-dimensional gauge glass,⁷ which has a continuous symmetry but is known to have a finite T_c .

The differences between DP and RSB can be quantified by studying the distribution^{4,8,9,10,11} $P(q)$ of the spin overlap q defined in Eq. (4) below. For finite systems, the DP predicts two peaks at $\pm q_{EA}$, where q_{EA} is the Edwards-Anderson order parameter, as well as a tail down to $q = 0$ that vanishes in the thermodynamic limit like^{12,13} $\sim L^{-\theta}$. On the contrary, RSB predicts a non-trivial distribution with a finite weight in the tail down to $q = 0$, independent of system size.

Earlier work that studied the nature of the spin-glass state has focused on the Ising spin glass,^{4,5,6,8} though some work has also been carried out on the gauge glass

model of the vortex glass transition in superconductors.⁷ Here, we consider a *vector spin-glass* model, the four-dimensional XY spin glass, which is known to have a finite transition temperature¹⁴ T_c with $T_c \simeq 0.95$. We perform Monte Carlo simulations for a modest range of sizes down to low temperatures ($T \simeq 0.2T_c$) using the parallel tempering Monte Carlo^{15,16} technique. Our main result is that that $P(0)$ does not appear to decrease with increasing system size for the range of sizes studied.

We also look for information on the surface of the large-scale low-energy excitations by studying the “link overlap” defined in Eq. (13) below. The data for this quantity suggests that the surface may be space filling, i.e., $d_s = d$, as in RSB, though the small range of sizes precludes us from making a firm statement on this and a scenario compatible with the DP is also viable in which $d_s < d$.

The layout of the paper is as follows: In Sec. II we describe the model and the measured observables. We discuss our equilibration tests for the parallel tempering Monte Carlo method for this specific model in Sec. III. Our results are discussed in Sec. IV. Section V summarizes our conclusions and presents ideas for future work.

II. MODEL AND OBSERVABLES

The XY spin glass consists of two-component spins of unit length on a hypercubic lattice in four dimensions with periodic boundary conditions. The Hamiltonian is given by

$$\mathcal{H} = - \sum_{\langle i,j \rangle} J_{ij} \mathbf{S}_i \cdot \mathbf{S}_j, \quad (1)$$

where the sum is over nearest neighbors, the linear size is L , the number of spins is $N = L^4$, and $\mathbf{S}_i \equiv (S_i^x, S_i^y)$ is an XY spin. Since $|\mathbf{S}_i| = 1$, one can parametrize the spins as $\mathbf{S}_i = [\cos(\phi_i), \sin(\phi_i)]$ with $\phi_i \in [0, 2\pi]$. The Hamiltonian then transforms to

$$\mathcal{H} = - \sum_{\langle i,j \rangle} J_{ij} \cos(\phi_i - \phi_j). \quad (2)$$

The J_{ij} are chosen according to a Gaussian distribution with zero mean and standard deviation J , i.e.,

$$\mathcal{P}(J_{ij}) = \frac{1}{\sqrt{2\pi}J} \exp\left[-\frac{J_{ij}^2}{2J^2}\right]. \quad (3)$$

Unless otherwise stated we will take $J = 1$.

We concentrate on two observables, the spin overlap q and the link overlap q_l . The (tensor) spin overlap is defined in terms of the spin configurations of two copies of the system, denoted by (1) and (2), as follows:

$$q_{\mu\nu} = \frac{1}{N} \sum_{i=1}^N S_{i,\mu}^{(1)} S_{i,\nu}^{(2)}, \quad \mu, \nu \in \{x, y\}. \quad (4)$$

In analytic work, the spin-glass order parameter is defined to be the average of the *trace* of $q_{\mu\nu}$. To be precise, for $L \rightarrow \infty$, the order parameter tensor is predicted to be of the form

$$\begin{pmatrix} q/2 & 0 \\ 0 & q/2 \end{pmatrix}. \quad (5)$$

However, this implicitly assumes that the symmetry has been broken by a small field, which is inconvenient to implement in numerics, so we adopt the following equivalent procedure. We apply all possible symmetries (rotations and reflection) to one replica and take the *largest* value of the resulting trace. Consider first rotations under which $q \rightarrow q'$ where

$$q' = \begin{pmatrix} q'_{xx} & q'_{xy} \\ q'_{yx} & q'_{yy} \end{pmatrix}. \quad (6)$$

Maximizing $\text{Tr}(q')$ with respect to the relative rotation angle between the replicas gives q_1 , where

$$q_1 = \sqrt{(q_{xx} + q_{yy})^2 + (q_{yx} - q_{xy})^2}. \quad (7)$$

The rotation also makes the two off-diagonal pieces equal, i.e., $q'_{xy} = q'_{yx}$.

We also must consider how the $q_{\mu\nu}$ transform under reflections of the angles of the spins in one replica, $\phi_i \rightarrow -\phi_i$. It is easy to see that under this transformation $q_1 \rightarrow q_2$ and vice-versa, where

$$\begin{aligned} q_2 &= \sqrt{(q'_{xx} - q'_{yy})^2 + (q'_{xy} + q'_{yx})^2} \\ &= \sqrt{(q_{xx} - q_{yy})^2 + (q_{xy} + q_{yx})^2}, \end{aligned} \quad (8)$$

where the second line follows after some algebra. Since the spin-glass order parameter is obtained by maximizing the trace with respect to all symmetry transformation, it is given by

$$q = \max\{q_1, q_2\}. \quad (9)$$

We use the notation q , somewhat inconsistently, for the spin-glass order parameter to conform with notation in

other work. The spin-glass order parameter function in RSB theory, $P(q)$, is given by the distribution of q in Eq. (9).

We also define the smaller of q_1 and q_2 by \bar{q} , i.e.,

$$\bar{q} = \min\{q_1, q_2\}. \quad (10)$$

If the order parameter tensor tends to the form in Eq. (5) for $L \rightarrow \infty$ then $\bar{q} \rightarrow 0$ in this limit. We shall see that our results support this.

If we are willing to *assume* that the form in Eq. (5) applies in the thermodynamic limit then we can obtain the spin glass order parameter distribution a little more simply from the quantity

$$Q = \sqrt{q_{xx}^2 + q_{yy}^2 + q_{yx}^2 + q_{xy}^2}, \quad (11)$$

which is invariant under symmetry transformations. Since

$$2Q^2 = q^2 + \bar{q}^2, \quad (12)$$

then, if $\bar{q} \rightarrow 0$ for $L \rightarrow \infty$, the distributions of q and $\sqrt{2}Q$ are the same in this limit.

The link overlap is defined, quite simply, by

$$q_l = \frac{1}{N_b} \sum_{\langle i,j \rangle} (\mathbf{S}_i^{(1)} \cdot \mathbf{S}_j^{(1)}) (\mathbf{S}_i^{(2)} \cdot \mathbf{S}_j^{(2)}), \quad (13)$$

where $N_b = Nd$ is the number of bonds ($d = 4$ is the space dimension). Since this is already invariant under global symmetry operations we do not need to consider the effects of rotations and reflections as we did for the spin overlap. The link overlap can be expressed in terms of spin angles by

$$q_l = \frac{1}{N_b} \sum_{\langle i,j \rangle} \cos(\phi_i^{(1)} - \phi_j^{(1)}) \cos(\phi_i^{(2)} - \phi_j^{(2)}). \quad (14)$$

While a change in q induced by flipping a cluster of spins is proportional to the *volume* of the cluster, q_l changes by an amount proportional to the *surface* of the cluster. The weight in $P(q)$ for small q varies as $L^{-\theta'}$, where θ' was introduced in Sec. I. In addition, we expect the variance of the link overlap to fit to a form $\text{Var}(q_l) \sim L^{-\mu_l}$ where, as shown in Ref. 8, $\mu_l = \theta' + 2(d - d_s)$.

III. EQUILIBRATION

For the simulations, we use the parallel tempering Monte Carlo method.^{15,16} In this technique, one simulates identical replicas of the system at N_T different temperatures, and, in addition to the usual local moves, one performs global moves where the temperatures of two replicas (with adjacent temperatures) are exchanged. This allows us to study larger systems at lower temperatures than with the conventional Monte Carlo method.

TABLE I: Parameters of the simulation. N_{samp} is the number of samples, i.e., sets of disorder realizations, N_{sweep} is the total number of sweeps simulated for each of the $2N_T$ replicas for a single sample, and N_T is the number of temperatures used in the parallel tempering method.

L	N_{samp}	N_{sweep}	N_T
3	1×10^4	3.0×10^4	39
4	2×10^3	4.0×10^5	39
5	1×10^3	2.0×10^6	39

Since we require two copies at each temperature to determine the spin and link overlaps, see Eqs. (4) and (13), we actually simulate $2N_T$ replicas.

The lowest temperature has to be far below $T_c \simeq 0.95$ and yet high enough that a range of sizes can be simulated. We chose the value of 0.2. The highest temperature has to be such that the system equilibrates very fast, and we chose 1.498. The intermediate temperatures are determined empirically provided that the acceptance ratios of the moves interchanging the replicas are larger than about 0.4 and are all roughly equal.

Table I lists the parameters of the simulation; N_{samp} (number of samples), N_{sweep} (total number of sweeps performed by each set of spins), and N_T (number of temperature values).

It is important to ensure that the system is equilibrated. However, the equilibration test proposed by Bhatt and Young¹⁷ does not work with parallel tempering Monte Carlo because the temperature of each replica does not stay constant throughout the simulation. Here we use the method introduced by Katzgraber *et al.*⁸ for short-range spin glasses with a Gaussian distribution of exchange interactions that relates the average energy to the link overlap. By performing an integration by parts with respect to J_{ij} of the average energy $U \equiv [\langle \mathcal{H} \rangle]_{\text{av}} (\leq 0)$, we obtain

$$[\langle q_l \rangle]_{\text{av}} = q_s - \frac{2T|U|}{zJ^2}, \quad (15)$$

where z is the number of nearest neighbors, $\langle \dots \rangle$ denotes a thermal average, and $[\dots]_{\text{av}}$ denotes an average over the disorder. The quantity q_s is given by

$$q_s = \frac{1}{N_b} \sum_{\langle i,j \rangle} [(\mathbf{S}_i \cdot \mathbf{S}_j)^2]_{\text{av}}, \quad (16)$$

where the sum is over pairs of neighboring spins. The simulation is started with randomly chosen spins so that all replicas are uncorrelated. This will have the effect that both sides of Eq. (15) are approached from opposite directions. Once they agree, the system is in equilibrium as can be seen in Fig. 1 for $T = 0.2$ (to be compared with $T_c \approx 0.95$),¹⁴ the lowest temperature simulated, and for $L = 3$. We show data for the smallest size since it allows us to generate more samples for longer equilibration times to better illustrate the method. For larger system sizes

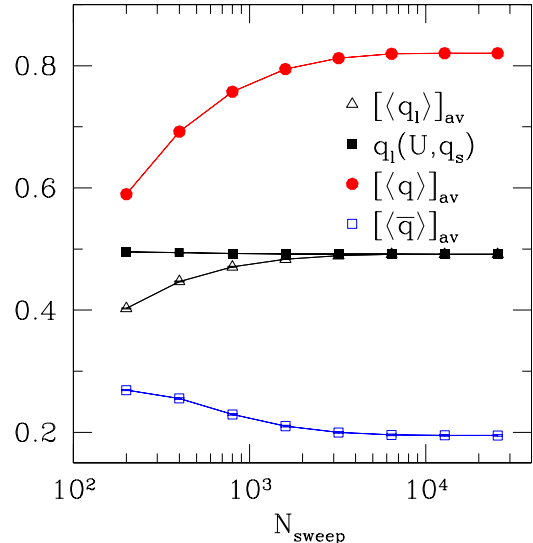


FIG. 1: A plot of $[\langle q_l \rangle]_{\text{av}}$ (the link overlap), $q_l(U, q_s)$ defined to be the RHS of Eq. (15), $[\langle q \rangle]_{\text{av}}$ the spin overlap, and $[\langle \bar{q} \rangle]_{\text{av}}$ defined in Eq. (10), as a function of Monte Carlo sweeps N_{sweep} for each replica, averaged over the last half of the sweeps. For equilibration, $[\langle q_l \rangle]_{\text{av}}$ and $q_l(U, q_s)$ should agree. The two sets of data approach each other from opposite directions and, once converged, do not seem to change at longer times, indicating that the system is equilibrated. The data for $[\langle q \rangle]_{\text{av}}$ and $[\langle \bar{q} \rangle]_{\text{av}}$ show that they too have equilibrated in roughly the same equilibration time. While not shown here, data for higher moments of the different observables have the same equilibration time as the link overlap $[\langle q_l \rangle]_{\text{av}}$. (Data for $L = 3$, $T = 0.2$, and 3230 samples).

we stop the simulation, once the data for $[\langle q_l \rangle]_{\text{av}}$ and the right-hand side (RHS) of Eq. (15) agree.

Because the XY spin glass has a vector order parameter symmetry, we discretize the angles of the spins to $N_\phi = 512$ to speed up the simulation. This number is large enough to avoid any crossover effects to other models as discussed by Cieplak *et al.*¹⁸. To ensure a reasonable acceptance ratio for single-spin Monte Carlo moves, we choose the proposed new angle for a spin within an acceptance window about the current angle, where the size of the window is proportional to the temperature T . By tuning a numerical prefactor, we ensure the acceptance ratios for these local moves are not smaller than 0.4 for each system size at the lowest temperature simulated.

IV. RESULTS

Figures 2 and 3 show data for $P(q)$ for $T = 0.20$ and 0.42, respectively. In both cases we see a peak at large q and a tail for smaller q that does not extend to $q = 0$. However, it is not surprising that there is a “hole” at

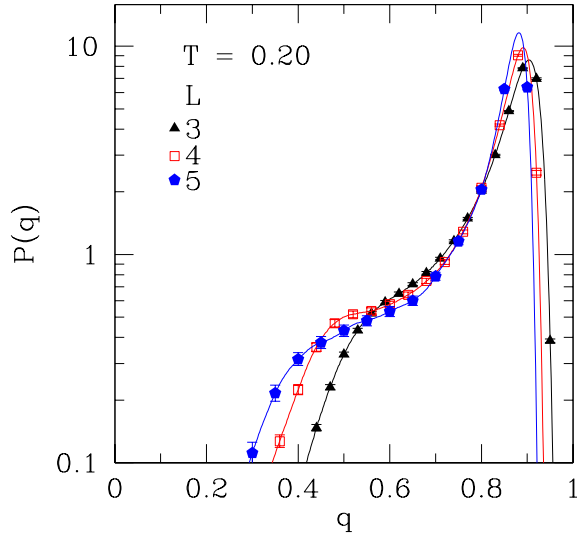


FIG. 2: Data for the spin overlap distribution $P(q)$ at temperature $T = 0.20$ for different system sizes. Note the logarithmic vertical scale. The lines go through all the data points but, for clarity, only some of the data points are shown.

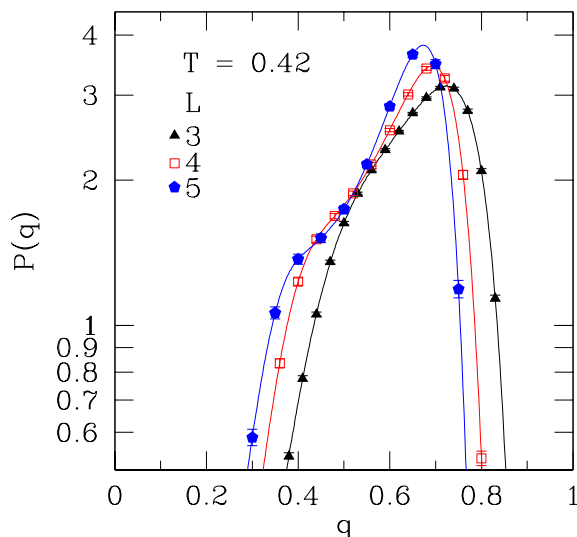


FIG. 3: Same as Fig. 2 but at temperature $T = 0.42$.

small q since q is defined to be the maximum of q_1 and q_2 . If $\bar{q} \equiv \min\{q_1, q_2\}$ tends to zero at large L , which is expected as discussed above, then, in RSB theory, the tail would extend to smaller values of q for larger L while maintaining the same height. Looking at Figs. 2 and 3, this seems to be the case, at least for the range of sizes

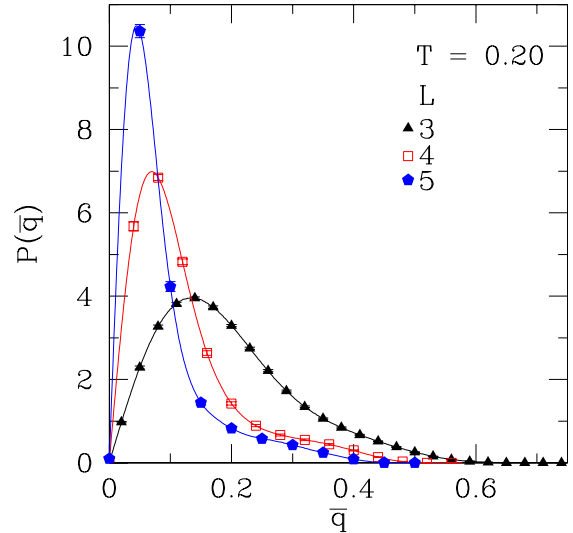


FIG. 4: Data for the overlap distribution $P(\bar{q})$ at temperature $T = 0.20$ for different system sizes. The weight in the distribution tends towards $\bar{q} = 0$ for increasing L .

that we have been able to study.

In Fig. 4 we show data for $P(\bar{q})$ at $T = 0.20$. As expected, the distributions seem to collapse to zero for increasing system size. Figure 5 shows the variation of the mean of \bar{q} with L on a log-log plot. The data have been fitted to straight lines with slopes shown. The quality of the fits¹⁹ is only moderate; $Q = 0.06, 0.09,$ and 0.04 for $T = 0.200, 0.247,$ and 0.305 , respectively. Given the rather small range of sizes, and hence the likelihood of systematic corrections to scaling, we feel that the data are consistent with $[\langle \bar{q} \rangle]_{\text{av}} \rightarrow 0$ for $L \rightarrow \infty$. Since $\bar{q} \geq 0$, if $[\langle \bar{q} \rangle]_{\text{av}} = 0$ then the whole distribution collapses to $\bar{q} = 0$.

Lastly we present in Figs. 6 and 7 results for the distribution of the link overlap $P(q_l)$. There is a pronounced peak at large q_l values as well as the hint of a shoulder for smaller values in the $T = 0.20$ data. The width of the distribution decreases with increasing system size. This is demonstrated in Fig. 8, which shows the variance of q_l against system size L for several low temperatures.

There is some curvature in the data for $\text{Var}(q_l)$, so first we attempt a three-parameter fit of the form

$$\text{Var}(q_l) = a + bL^{-c}, \quad (17)$$

finding small but finite values for a , see Table II. As we have the same number of data points as variables, we cannot assign fitting probabilities to the fits. We also attempt a power-law fit of the form

$$\text{Var}(q_l) = dL^{-\mu_l}, \quad (18)$$

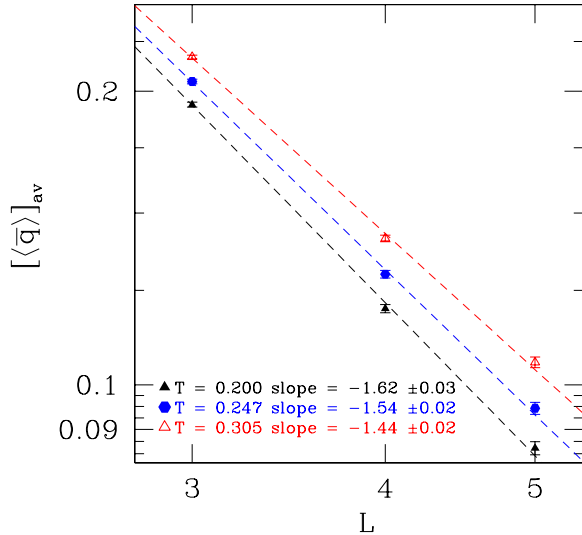


FIG. 5: Log-log plot of $[\langle \bar{q} \rangle]_{av}$ as a function of system size L at several temperatures.

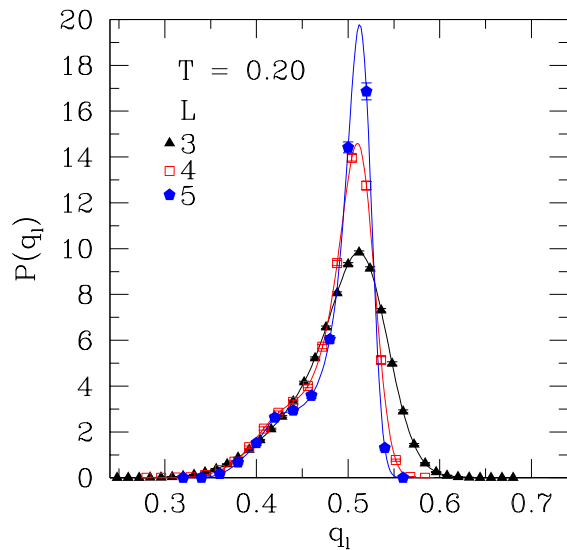


FIG. 6: The distribution of the link overlap at $T = 0.20$ for different sizes.

see Table III. However, the quality of the fits is poor as shown by the fitting probabilities¹⁹ Q . The effective exponent μ_l is found to vary with temperature. Extrapolating to $T = 0$, we obtain $\mu_l \equiv \theta' + 2(d - d_s) = 0.294 \pm 0.073$. If we assume that $\theta' \approx 0$, this gives $d - d_s = 0.147 \pm 0.036$.

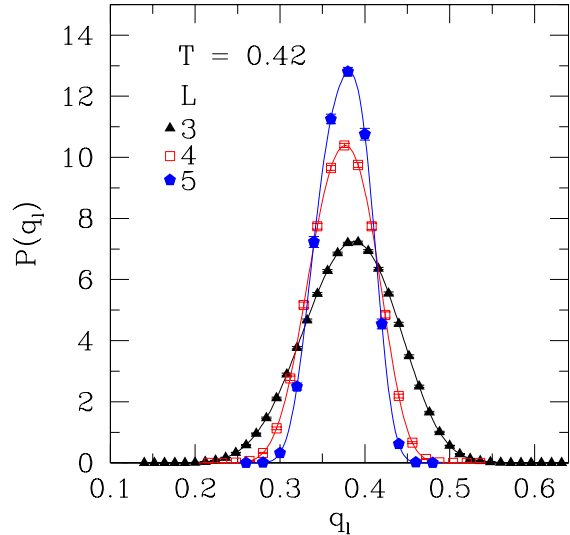


FIG. 7: Same as Fig. 6 but at temperature $T = 0.42$.

TABLE II: Fits for $\text{Var}(q_l)$. Fit parameters for the fit in Eq. (17) for different temperatures. We cannot quote fitting probabilities since we have the same number of data points as variables.

T	a	b	c
0.200	0.00100	0.0205	2.55
0.247	0.00087	0.0328	2.76
0.305	0.00073	0.0611	3.16
0.420	0.00036	0.1044	3.40

V. CONCLUSIONS

To conclude, we have studied the low-temperature properties of the four-dimensional XY spin glass at low temperatures. Our main result is that the order parameter distribution $P(q)$ has, in addition to a peak, a tail that seems to extend for smaller values of q , and whose height seems to persist, as the system size increases, see Figs. 2 and 3. This interpretation of the data is compatible with the RSB picture or the KMPY scenario. How-

TABLE III: Fit parameters for the fit in Eq. (18) for different temperatures. Note that the fit probabilities Q are small.

T	d	μ_l	Q
0.200	-4.92 ± 0.06	1.07 ± 0.05	5.0×10^{-2}
0.247	-4.50 ± 0.05	1.38 ± 0.04	3.6×10^{-3}
0.305	-3.99 ± 0.04	1.77 ± 0.03	2.9×10^{-6}
0.420	-3.06 ± 0.04	2.56 ± 0.03	6.0×10^{-8}

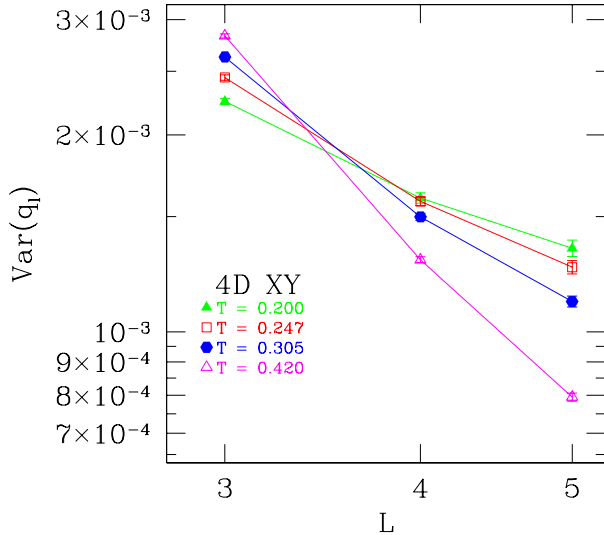


FIG. 8: Log-log plot of the variance of q_l as a function of system size L at several temperatures.

ever, the range of lattice sizes is very small, so it is not clear if this interpretation would persist to large sizes. Unfortunately, it is currently not feasible to study much larger sizes in equilibrium, because relaxation times are too long. Nonetheless, we feel that results on rather small equilibrated samples are of interest in their own right for the following reason: In any experiment, a sample is not

fully equilibrated at low temperatures, but is rather only equilibrated up to some finite length scale, which only increases slowly with increasing measurement time. Thus a complete understanding will require a *nonequilibrium theory*, but a component of this is likely to be a theory of equilibrium on *finite* scales where local equilibrium has been achieved.

We have also studied the link overlap q_l . The variance of q_l decreases with increasing L but we are unable to ascertain whether it tends to zero in the thermodynamic limit, and hence we are unable to determine whether or not the surface is space filling.

In future work, it would be useful to look more carefully at the nature of the large-scale low-energy excitations to see whether they correspond to gradual orientations in the spin directions or whether vortices play a role.

Acknowledgments

This work was supported by the National Science Foundation under grant No. DMR 0086287. We are grateful to D. A. Huse for correspondence about the possible role of vortices. The numerical calculations were made possible by use of the UCSC Physics graduate computing cluster funded by the Department of Education Graduate Assistance in the Areas of National Need program. We would also like to thank the University of New Mexico for access to their Albuquerque High Performance Computing Center. This work utilized the UNM-Truchas Linux Clusters.

* Electronic address: dummkopf@physics.ucsc.edu; Present address: Department of Physics, University of California, Davis, California 95616

† Electronic address: peter@bartok.ucsc.edu; URL: <http://bartok.ucsc.edu/peter>; Present address: Department of Theoretical Physics, 1, Keble Road, Oxford OX1 3NP, England

¹ D. S. Fisher and D. A. Huse, J. Phys. A. **20**, L997 (1987); D. A. Huse and D. S. Fisher, J. Phys. A. **20**, L1005 (1987); D. S. Fisher and D. A. Huse, Phys. Rev. B **38**, 386 (1988).

² G. Parisi, Phys. Rev. Lett. **43**, 1754 (1979); J. Phys. A **13**, 1101, (1980); Phys. Rev. Lett. **50**, 1946 (1983).

³ M. Mézard, G. Parisi, and M. A. Virasoro, *Spin Glass Theory and Beyond* (World Scientific, Singapore, 1987).

⁴ E. Marinari, G. Parisi, F. Ricci-Tersenghi, J. Ruiz-Lorenzo, and F. Zuliani, J. Stat. Phys. **98**, 973 (2000).

⁵ F. Krzakala and O. C. Martin, Phys. Rev. Lett. **85**, 3013 (2000).

⁶ M. Palassini and A. P. Young, Phys. Rev. Lett. **85**, 3017 (2000).

⁷ H. G. Katzgraber and A. P. Young, Phys. Rev B **64**, 104426 (2001).

⁸ H. G. Katzgraber, M. Palassini, and A. P. Young, Phys.

Rev. B **63**, 184422, (2001).

⁹ J. D. Reger, R. N. Bhatt, and A. P. Young, Phys. Rev. Lett. **64**, 1859 (1990).

¹⁰ E. Marinari, G. Parisi, and J. J. Ruiz-Lorenzo, in *Spin Glasses and Random Fields*, edited by A. P. Young (World Scientific, Singapore, 1998), and references therein.

¹¹ E. Marinari and F. Zuliani, J. Phys. A **32**, 7447 (1999).

¹² A. J. Bray and M. A. Moore, in *Heidelberg Colloquium on Glassy Dynamics and Optimization*, edited by L. Van Hemmen and I. Morgenstern (Springer-Verlag, Berlin, 1986), p. 121.

¹³ M. A. Moore, H. Bokil, and B. Drossel, Phys. Rev. Lett. **81**, 4252 (1998).

¹⁴ S. Jain, J. Phys. A **29**, L385 (1996).

¹⁵ K. Hukushima and K. Nemoto, J. Phys. Soc. Jpn. **65**, 1604 (1996).

¹⁶ E. Marinari, in *Advances in Computer Simulation*, edited by J. Kertész and Imre Kondor (Springer Verlag, Berlin 1998), p. 50, (cond-mat/9612010).

¹⁷ R. N. Bhatt and A. P. Young, Phys. Rev. Lett. **54**, 924 (1985); Phys. Rev. B **37**, 5606 (1988).

¹⁸ M. Cieplak, J. R. Banavar, M. S. Li, and A. Khurana, Phys. Rev. B **45**, 786 (1992).

- ¹⁹ W. H. Press, S. A. Teukolsky, W. T. Vetterling, and B. P. Flannery, *Numerical Recipes in C* (Cambridge University Press, Cambridge, England, 1995).